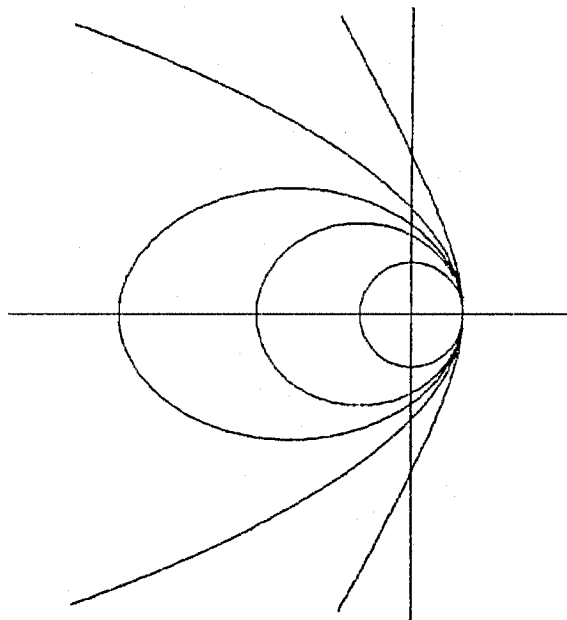


RELATING CONIC-SECTION ORBITAL POSITION, VELOCITY,
AND TIME FROM PERIAPSIS AS DIMENSIONLESS QUANTITIES

J. Phil Barnes

Northrop Aircraft Division



AAS/AIAA Astrodynamics Specialist Conference

KALISPELL, MONTANA AUGUST 10 - 13, 1987

AAS Publications Office, P.O. Box 28130, San Diego, CA 92128

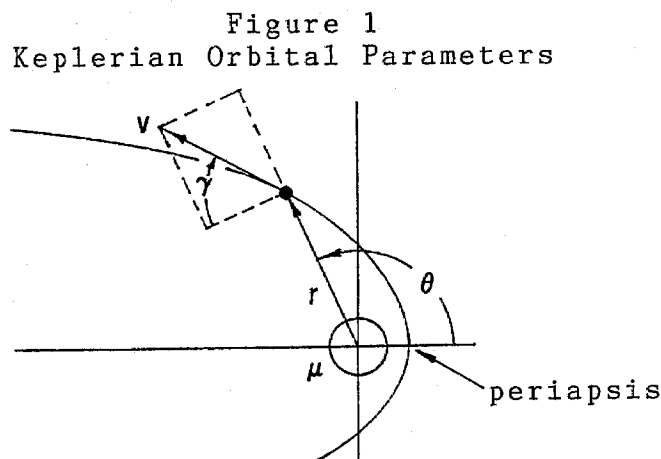
RELATING CONIC-SECTION ORBITAL POSITION, VELOCITY,
AND TIME FROM PERIAPSIS AS DIMENSIONLESS QUANTITIES

J. Phil Barnes*

Keplerian orbital characteristics are presented in compact mathematical and graphical form by non-dimensionalizing orbital radius, velocity, energy, and time from periapsis. The auxiliary anomalies are used to obtain the dimensionless time. The accuracies of the eccentric and hyperbolic anomalies are confirmed, particularly at near-parabolic eccentricity, by numerical solution of Kepler's problem. Finally, the dimensionless groups are applied toward analysis of a lunar free-return trajectory via the patched-conic method with the aid of Cartesian vector operations.

INTRODUCTION

A Keplerian orbit (Figure 1) has the shape of a conic section. The orbit is defined by its eccentricity (e), angular momentum (h) per unit satellite mass, and central body gravitational parameter (μ). The orbital radius (r), velocity (v), and time (t) from periapsis can be multiplied by various powers of (μ) and (h) to form dimensionless groups which, along with flight-path angle (γ), depend only on the eccentricity and true anomaly (θ). The orbital energy (\mathcal{E}) per unit satellite mass can also be non-dimensionalized.



The dimensionless groups, derived in Appendix 1, are summarized as follows, using upper-case letters (R, V, E, and T) to designate non-dimensionality:

* Senior Engineer, Northrop Aircraft Division

Introduction, continued

$$\text{Radius Group} \quad R = r\mu/h^2 = 1/(1 + e \cos \theta)$$

$$\text{Velocity Group} \quad V = vh/\mu = \sqrt{1 + e^2 + 2e \cos \theta}$$

$$\text{Flight-Path Angle} \quad \gamma = \cos^{-1}(1/RV)$$

$$\text{Energy Group} \quad E = \epsilon h^2/\mu^2 = \frac{1}{2}(V^2) - (1/R) = \frac{1}{2}(e^2 - 1)$$

$$\text{Time Group} \quad T = t\mu^2/2\pi h^3 = (1/2\pi) \int_0^\theta \frac{d\theta}{(1 + e \cos \theta)^2}$$

Since the time-group integral cannot be evaluated by ordinary means (unless $e=1$), the eccentric anomaly (ϵ) and hyperbolic anomaly (F) were devised (Ref.1) as auxiliary anomalies which can be integrated. For eccentric, parabolic, and hyperbolic orbits, the time group is respectively as follows:

* After this paper was written, it was found that the time group can be integrated, as in Thomson's book, "Introduction to Space Mechanics," Dover, 1986, page 73.

$$\text{For } e < 1, \quad T = \frac{\epsilon - e \sin \epsilon}{2\pi (1 - e^2)^{3/2}}$$

$$\text{For } e = 1, \quad T = \frac{3 \tan(\frac{1}{2}\theta) + \tan^3(\frac{1}{2}\theta)}{12\pi}$$

$$\text{For } e > 1, \quad T = \frac{e \sinh(F) - F}{2\pi (e^2 - 1)^{3/2}}$$

With the auxiliary anomalies (ϵ , $\frac{1}{2}\theta$, or F) the solution of Kepler's problem (to determine θ , given T) is iterative. Also, when the eccentricity is near unity the iterative solutions are slow to converge and may be subject to error when (T) is evaluated in single precision. As an alternate, non-iterative solution to Kepler's problem, the dimensionless time derivative ($d\theta/dT$) can be integrated numerically:

$$d\theta/dT = 2\pi (1 + e \cos \theta)^2 \longrightarrow \theta \approx \sum_0^T (d\theta/dT) \Delta T$$

The numerical integration can be used to test the accuracy of (T) as determined by the auxiliary anomalies. Also, numerical integration can be used as an alternative to the iterative methods when they are slow or unable to converge.

Regardless of how the time group (T) is obtained, the dimensionless groups (R, V, E , and T) offer compact presentation of orbital characteristics, as well as efficient analysis of conic and patched-conic orbits.

PRESENTATION OF ORBITAL CHARACTERISTICS

The orbital shapes can be compared by plotting dimensionless Cartesian coordinates, $X=R\cos\theta$ and $Y=R\sin\theta$, as shown in Figure 2. As might be expected, the circular orbit has a radius group of unity. At the semilatus nodes, all conic orbits have a radius group of unity. By scaling up the X-Y coordinates by the factor $(1+e)$, the orbits can be compared with common periapsis as shown in Figure 3.

The velocity group, as well, is unity in a circular orbit (Figure 4). In eccentric orbits, the velocity group is $(1+e)$ at periapsis and $(1-e)$ at apoapsis. The direction of the velocity vector is given by the flight-path angle (γ), which varies with (e, θ) as shown in Figure 5. In hyperbolic orbits (Figure 6) the velocity group is again $(1+e)$ at periapsis. The flight-path angle is linear with true anomaly for a parabolic orbit (Figure 7).

For eccentric, parabolic, and hyperbolic orbits the dimensionless time from periapsis (time group, T) is presented in Figure 8. Note that the dimensionless period of the circular orbit is unity. The time group arbitrarily contains (2π) in its definition, allowing convenient cancellation of the (2π) when converting radians to degrees in numerical or iterative solutions to Kepler's problem.

For eccentric orbits, the period (τ) and period group (P) are related as follows:

$$P = \tau \mu^2 / 2 \pi h^3 = 1 / (1-e^2)^{3/2}$$

Figure 9 relates the true anomaly to the time from periapsis as a fraction (t/τ) of the period.

In hyperbolic orbits (Figure 10) the time group is negative approaching periapsis. Figures 8 or 10 can be used for approximate graphical solution of Kepler's problem. Given an initial true anomaly (θ_1) along with the eccentricity, the initial time group (T_1) can be obtained graphically. Then, given (h) and (μ) , the time interval (t_2-t_1) is non-dimensionalized to form (T_2-T_1) . Then, given the final time group (T_2), the final true anomaly (θ_2) is obtained graphically.

Figures 8 or 10 also offer a close first guess for the final true anomaly in the iterative solution to Kepler's problem, as illustrated in Appendix 2. Since the iterative solution uses (e) , (T) , and the auxiliary anomaly to determine (θ) , the velocity group ($V=vh/\mu$) is ideally suited for determining the dimensional velocity (v):

$$v = (\mu/h) \sqrt{1+e^2+2e\cos\theta}$$

(3)

Figure 2

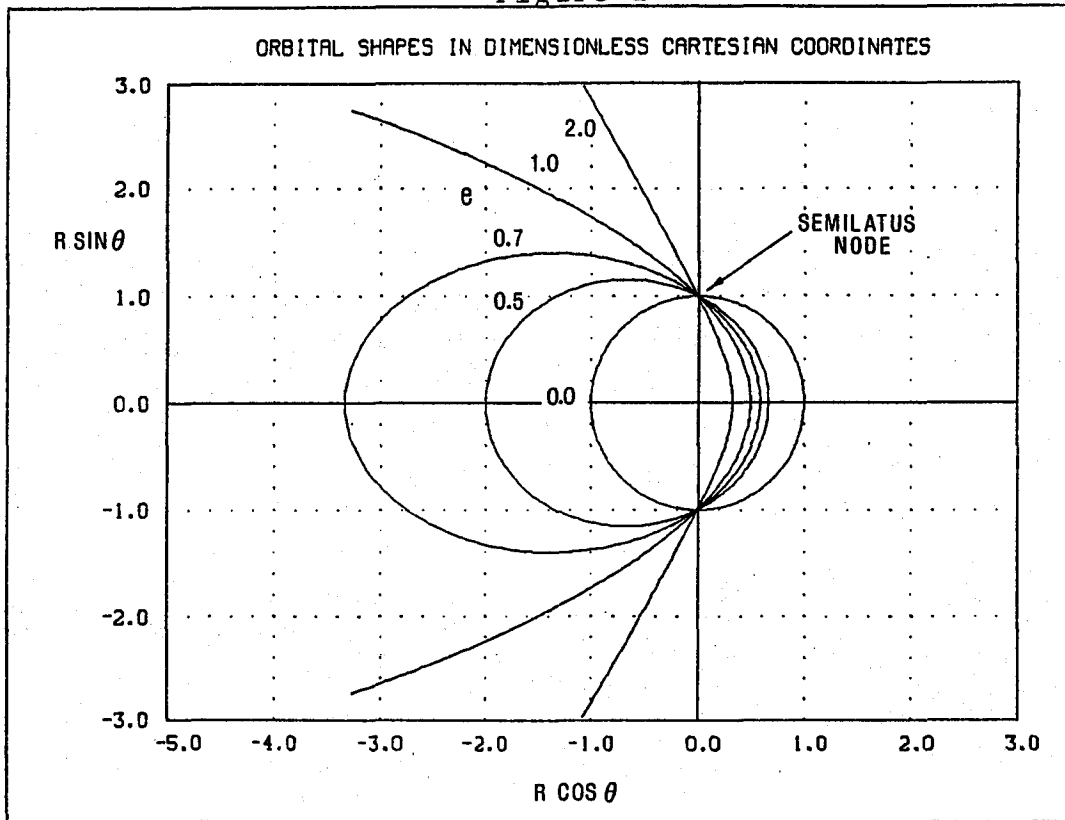


Figure 3

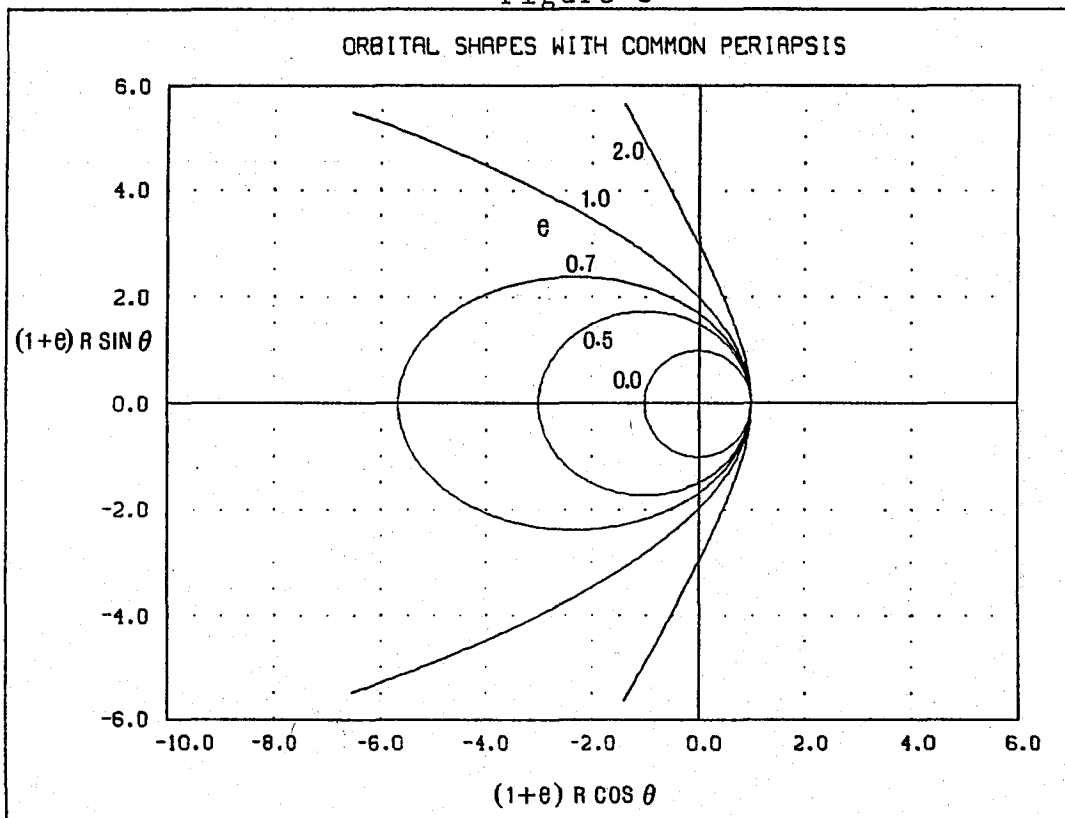


Figure 4

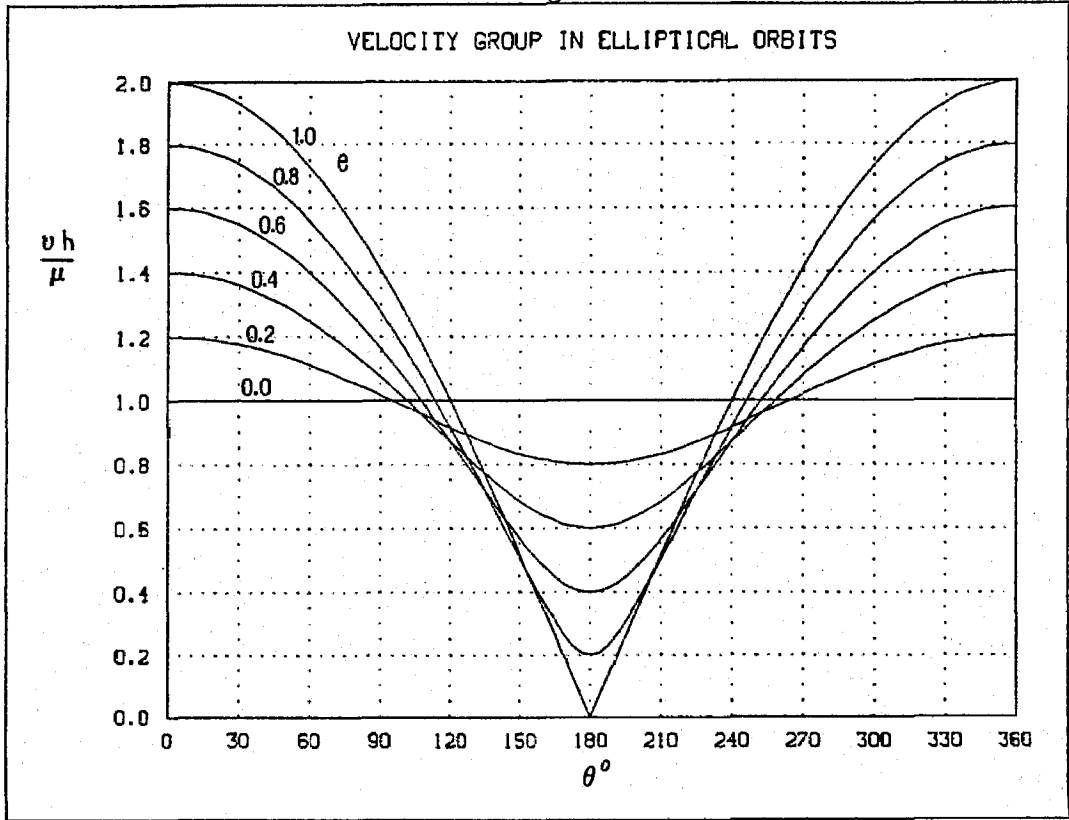


Figure 5

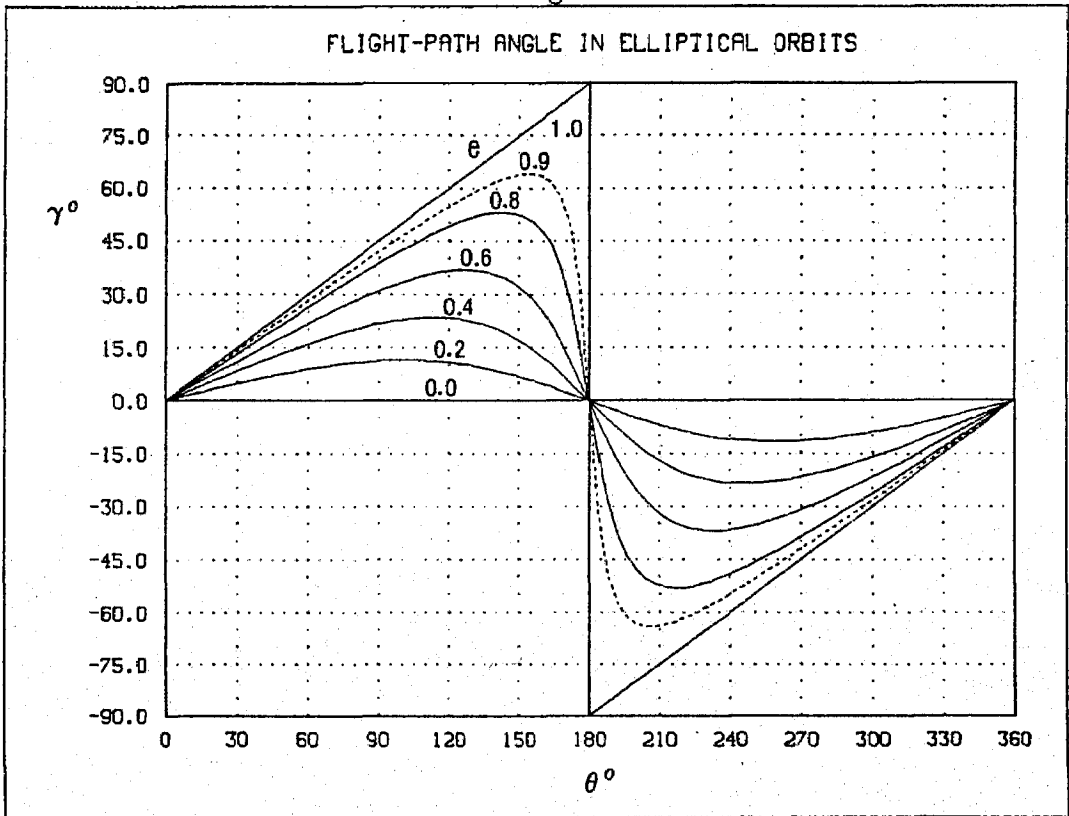


Figure 6

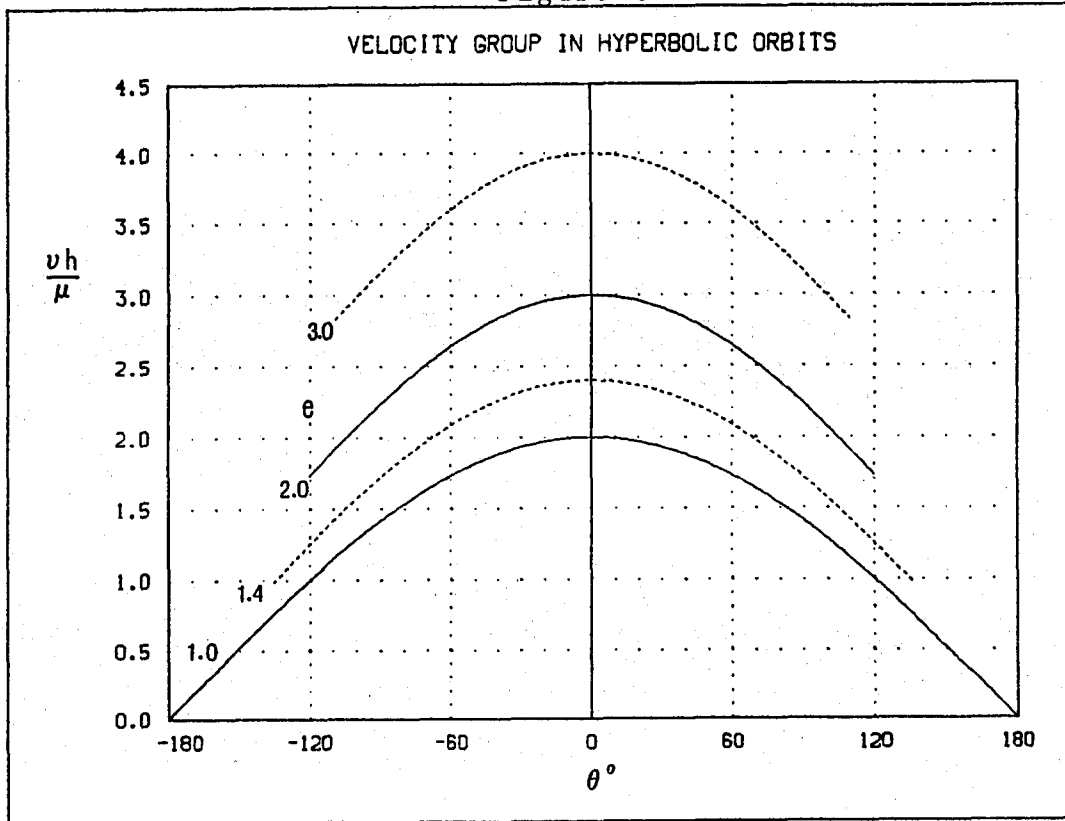


Figure 7

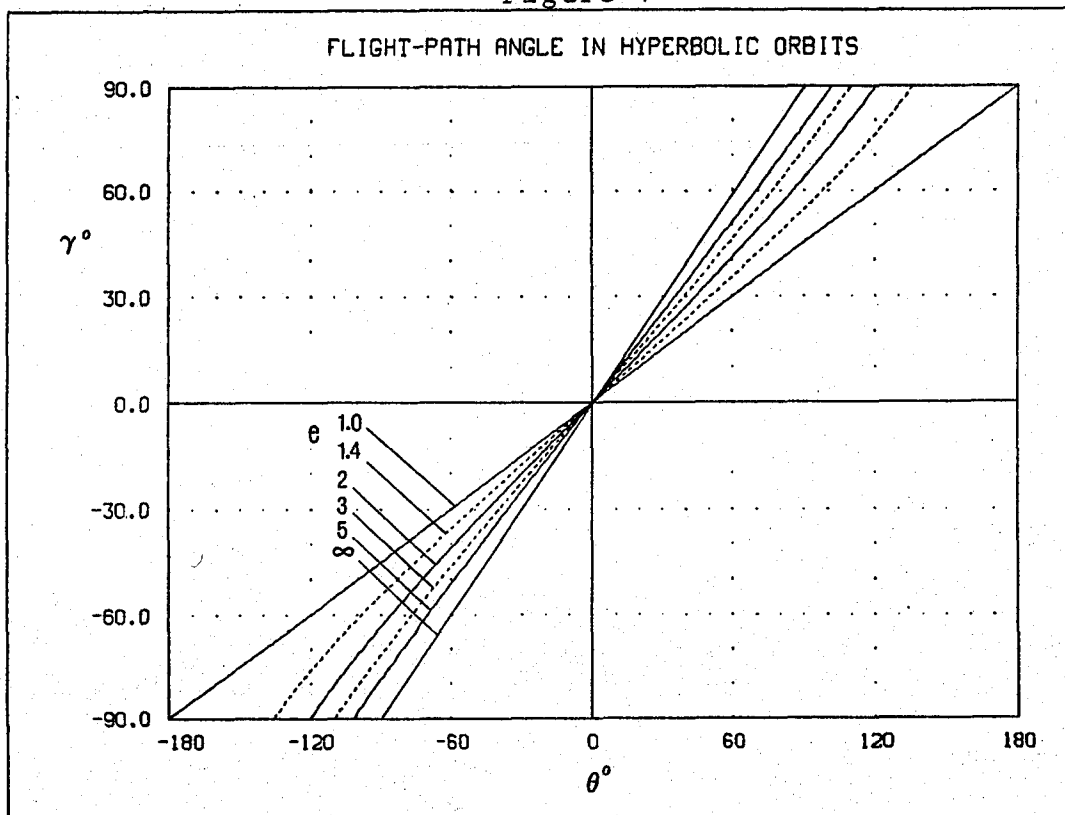


Figure 8

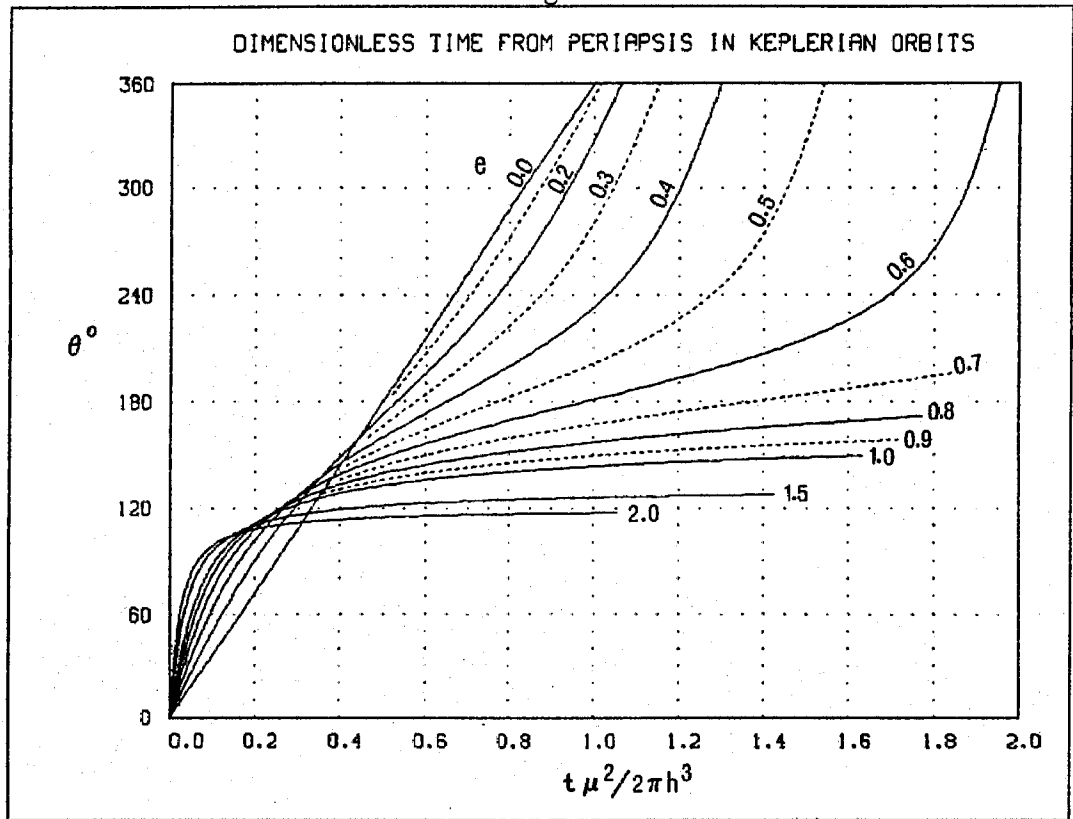


Figure 9

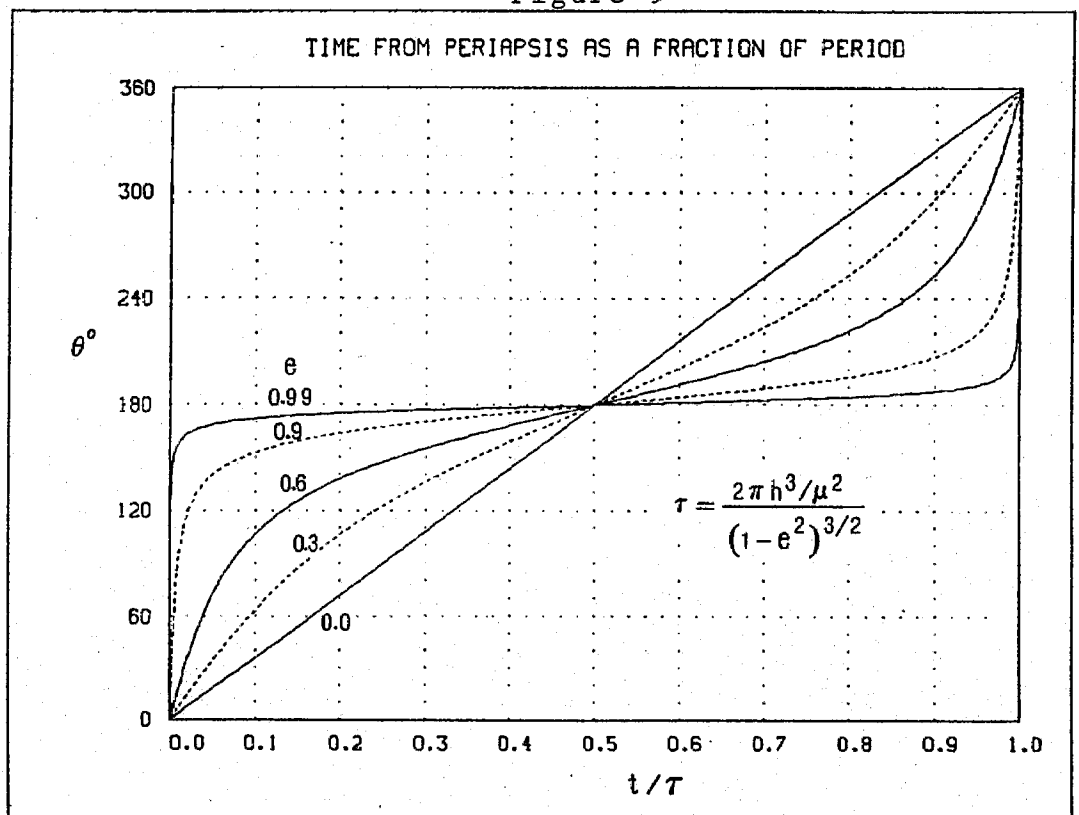
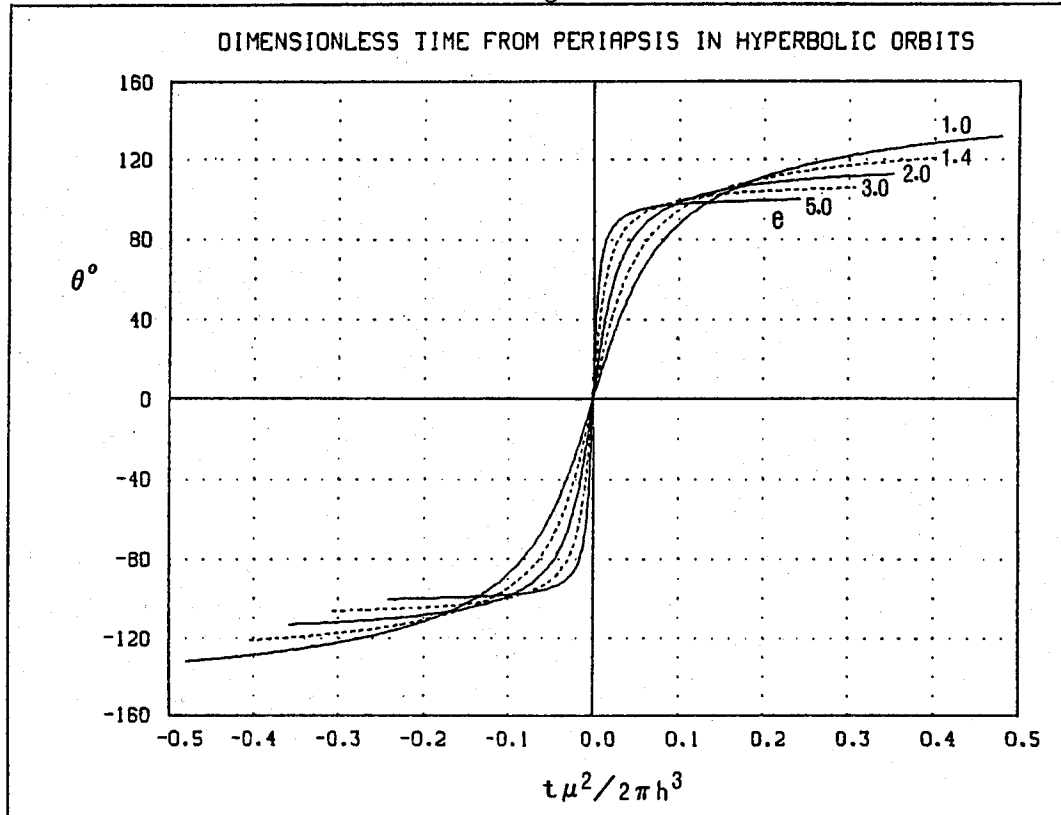


Figure 10



NUMERICAL SOLUTION OF KEPLER'S PROBLEM

The dimensionless time (T) from periapsis to any true anomaly (θ) is given by:

$$T = t\mu^2/2\pi h^3 = (1/2\pi) \int_0^\theta \frac{d\theta}{(1+e\cos\theta)^2}$$

The integral can be evaluated numerically, with Simpson's Rule for example, to determine (T), given (e) and (θ). The result can be used to check the accuracy of (T) as determined by the auxiliary anomalies. Alternatively, the equation above can be differentiated and rearranged to yield the dimensionless time derivative:

$$d\theta/dT = 2\pi(1+e\cos\theta)^2$$

This derivative can be used to numerically solve Kepler's problem with a constant or variable time group increment (ΔT). In Table 1, the Runge-Kutta method (Appendix 3) was used with variable (ΔT) adjusted to advance roughly $1^\circ \approx (\theta_{i+1} - \theta_i)$ in true anomaly at each step:

$$\Delta T = T_{i+1} - T_i = 1^\circ (2\pi/360^\circ) / [2\pi(1+e\cos\theta_i)^2]$$

The actual advance ($\theta_{i+1} - \theta_i$) was calculated in double precision with the Runge-Kutta method. Then, given (θ), the auxiliary anomaly was used to calculate (T) in double precision, thereby obtaining a comparison of the methods at each step.

Table 1
Time Group Comparison
Double Precision

e	θ°	$\tau = t\mu^2/2\pi h^3$	
	TRUE ANOMALY	NUMERICAL \times INTEGRATION	AUXILIARY ANOMALY
0.6	44.8852	.0527286	.0527286
0.6	89.5376	.1377633	.1377632
0.6	178.619	.9525895	.9525893
0.6	181.619	1.004654	1.004654
0.99	44.8450	.0350285	.0350284
0.99	89.3285	.1048998	.1048998
0.99	136.083	.5895153	.5895152
0.99	169.745	21.21108	21.21114
0.99	180.815	200.6112	200.6123
0.999	44.8443	.0347316	.0347316
0.999	137.975	.6735287	.6735285
0.999	170.263	40.55587	40.55624
0.999	176.669	615.5090	615.7290
0.999	178.914	2885.342	2888.557
0.999	180.767	7605.110	7608.113
1.0	59.7174	.0507011	.0507011
1.0	123.518	.3193351	.3193350
1.0	165.897	14.65918	14.65920
1.0	174.244	210.3356	210.3592
1.001	59.7172	.0506562	.0506562
1.001	123.516	.3195205	.3195204
1.001	165.870	15.13996	15.13998
1.001	170.160	46.13354	46.13406
2.0	59.6042	.0244402	.0244402
2.0	93.7751	.0778429	.0778429
2.0	116.732	.8392446	.8392227

* VARIABLE TIME GROUP INCREMENT $\Delta T = 1^\circ / (d\theta/dT)$

The results of the numerical integration are seen to agree with those of the auxiliary anomaly generally to five or more significant digits, except at the far side of a highly-eccentric orbit ($e \approx 0.999$, $\theta \approx 180^\circ$) where the methods differ at the fourth significant digit. All computations in Table 1 are non-iterative. The computations using the auxiliary anomaly were non-iterative because (θ) was specified. If, however, (T) were specified and (θ) were to be iteratively determined, convergence on (θ) may not be reliable when using the auxiliary anomaly at near-parabolic eccentricity. In this case, numerical integration offers a reliable, non-iterative solution for (θ) accurate to a small fraction of 1° .

When computations are limited to single precision, the numerical integration is frequently more accurate than the auxiliary anomaly at near-parabolic eccentricity. Table 2 presents an accuracy comparison, using the auxiliary anomaly in double precision as the standard of accuracy, and dots to indicate the more accurate values of (T).

TABLE 2
TIME GROUP ACCURACY COMPARISON
SINGLE PRECISION

e	θ° TRUE ANOMALY	$T = t\mu^2/2\pi h^3$		
		NUMERICAL * INTEGRATION	AUXILIARY ANOMALY	EXACT **
0.99	9.9926	0.007044	0.007044	0.007044
0.99	59.718	0.051152 •	0.051148	0.051152
0.99	120.62	0.281475	• 0.281471	0.281469
0.99	175.12	67.19261	• 67.19213	67.19140
0.99	179.80	172.7628	• 172.7603	172.7578
0.999	9.9926	0.006981 •	0.006978	0.006981
0.999	59.717	0.050745 •	0.050749	0.050745
0.999	119.63	0.271576 •	0.271621	0.271571
0.999	170.26	40.52766 •	40.53115	40.52691
0.999	178.15	1678.677	• 1680.191	1680.005
0.999	180.76	7596.878	• 7599.535	7599.068
1.0	29.931	0.021778	0.021778	0.021778
1.0	90.305	0.106958	• 0.106957	0.106957
1.0	150.31	1.725030	• 1.724981	1.724975
1.0	175.71	509.8093	• 509.9658	509.9817
1.01	4.9982	0.003440 •	0.003383	0.003440
1.01	29.931	0.021567 •	0.021575	0.021567
1.01	90.300	0.106311 •	0.106314	0.106310
1.01	150.24	1.840474	• 1.840397	1.840426
1.01	170.84	289.2851	• 289.7937	289.7665
1.001	9.9926	0.006967 •	0.006961	0.006967
1.001	29.931	0.021757 •	0.022442	0.021757
1.001	60.707	0.051882 •	0.052735	0.051882
1.001	90.305	0.106893 •	0.107820	0.106892
1.001	120.60	0.282638 •	0.283232	0.282631
1.001	150.30	1.735943 •	1.736358	1.735899
1.001	170.15	46.09414	• 46.09236	46.09021
1.001	175.49	693.5461	• 694.2402	693.9728

* VARIABLE TIME GROUP INCREMENT

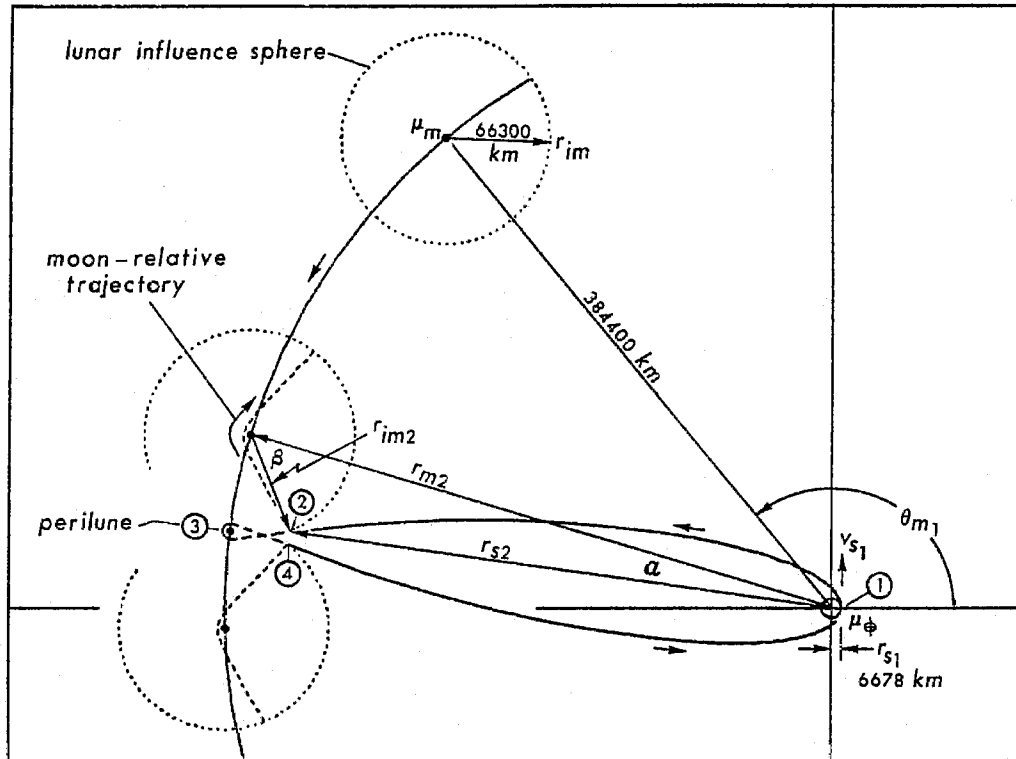
** AUXILIARY ANOMALY IN DOUBLE PRECISION

ORBIT ANALYSIS WITH THE DIMENSIONLESS GROUPS

To illustrate the application of the dimensionless groups, a lunar free-return trajectory (Figure 11) will be analyzed with the patched-conic method (Ref. 2). The free-return trajectory is useful in the event that the decelerating impulse is not available at perilune, because lunar gravity will then swing the spacecraft into a trajectory returning to the same perigee altitude as the outbound trip.

The patched-conic method can be used for approximate analysis of the free-return trajectory. With this method, the trajectory is analyzed by patching together the various 2-body (conic) orbits, neglecting the effects of third bodies. In the lunar free-return trajectory, only the earth's gravity ($\mu_E=398601 \text{ km}^3/\text{s}^2$) is considered until the spacecraft enters the lunar sphere of influence at a distance ($r_{im}=66300 \text{ km}$) from the moon. Within the lunar influence sphere ($\mu_m=4903 \text{ km}^3/\text{s}^2$), the effects of the earth on the moon-relative trajectory are neglected. Furthermore, the effects of the sun are neglected in both patched orbits.

Figure 11
Lunar Free-Return Trajectory



The spacecraft is injected at point (1) from a geocentric parking orbit of 300 km altitude into a highly-eccentric transfer crossing in front of the moon's path. At point (2) the spacecraft enters the lunar influence sphere, beginning its moon-relative hyperbolic encounter. The spacecraft reaches perilune at point (3) and then leaves the lunar influence sphere at point (4). The objectives are to determine the injection speed (v_{s1}), phase angle (θ_{m1}), time (t_{13}) to perilune, and perilune altitude, all such that the earth-relative eccentricity and energy of the return trip match those of the outbound trip.

The analysis begins as recommended in Ref. 1, where both (v_{s1}) and the intercept angle (β) are estimated. These estimates are later revised if the desired trajectory is not observed. From (v_{s1}) and (r_{s1}) the earth-relative angular momentum (h_{12}) is determined. Then the velocity group (V_{s1}) and eccentricity (e_{12}) are determined. From (β , r_{m2} , and r_{im2}) the law of cosines is applied to determine the radius (r_{s2}). Then the radius group (R_{s2}) and true anomaly (θ_{s2}) are calculated:

$$h_{12} = r_{s1} v_{s1} \quad (\text{at periapsis})$$

$$V_{s1} = v_{s1} h_{12} / \mu_\phi$$

$$e_{12} = V_{s1} - 1 \quad (\text{at periapsis})$$

$$R_{s2} = r_{s2} \mu_\phi / h_{12}^2$$

(11)

$$\theta_{s2} = \cos^{-1}[(1/e_{12})(1/R_{s2}-1)]$$

Next, the velocity group (V_{s2}), velocity (v_{s2}), flight-path angle (γ_{s2}), and velocity vector components are calculated (Refer to Figure 11a):

$$V_{s2} = \sqrt{1+e_{12}^2+2 e_{12}\cos\theta_{s2}}$$

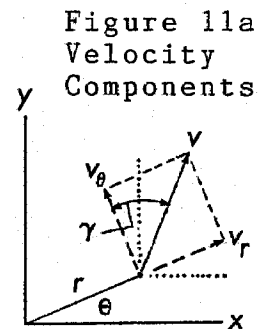
$$v_{s2} = V_{s2}\mu_{\oplus}/h_{12}$$

$$\gamma_{s2} = \cos^{-1}(1/R_{s2}V_{s2})$$

$$v_{s2\theta} = v_{s2} \cos\gamma_{s2}; \quad v_{s2r} = v_{s2} \sin\gamma_{s2}$$

$$v_{s2x} = v_{s2r} \cos\theta_{s2} - v_{s2\theta} \sin\theta_{s2}$$

$$v_{s2y} = v_{s2r} \sin\theta_{s2} + v_{s2\theta} \cos\theta_{s2}$$



To determine the lunar velocity vector (\bar{v}_{m2}) the law of sines is used to determine the angle (α), which is then subtracted from (θ_{s2}) to obtain (θ_{m2}). Then the x-y components of (\bar{v}_{m2}) can be determined. The lunar velocity vector is subtracted from the spacecraft velocity vector to obtain the relative velocity vector (\bar{v}_{s2m}) with which the spacecraft begins its hyperbolic passage. The lunar influence radius, as a vector (\bar{r}_{im2}), is calculated by subtracting the vector (\bar{r}_{s2}) from (\bar{r}_{m2}) using x-y components ($r \cos\theta$) and ($r \sin\theta$). Finally, the moon-relative angular momentum is found by the vector cross product:

$$\text{vector: } \bar{h}_{24} = \bar{r}_{im2} \times \bar{v}_{s2m}$$

$$\text{scalar: } h_{24} = r_{im2x} v_{s2my} - r_{im2y} v_{s2mx}$$

The scalar angular momentum (h_{24}) will be negative, provided the spacecraft passes in front of the moon. Taking note of the sign of (h_{24}) for use in subsequent vector rotation operations, its absolute value is used for all remaining calculations. The moon-relative radius group, velocity group, energy group, and eccentricity are as follows:

$$R_{s2m} = r_{im} \mu_m / h_{24}^2$$

$$V_{s2m} = v_{s2m} h_{24} / \mu_m$$

$$E_{24} = \frac{1}{2}(V_{s2m})^2 - (1/R_{s2m})$$

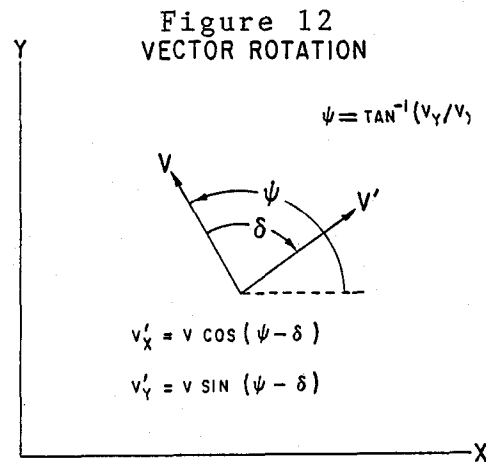
$$e_{24} = \sqrt{2E_{24}+1}$$

The spacecraft enters the lunar influence sphere with an initial true anomaly:

$$\theta_{s2m} = -\cos^{-1}[(1/e_{24})(1/R_{s2m}-1)]$$

The moon-relative true anomaly (θ_{s4m}) at exit from the lunar influence sphere is positive, with magnitude (θ_{s2m}). Thus, the moon-to-spacecraft radius vector sweeps out an angle ($2\theta_{s4m}$) during hyperbolic passage. This rotation is clockwise, provided the scalar angular momentum (h_{24}) was originally of negative sign. The moon-spacecraft radius vector (\bar{r}_{im4}) can thus be determined by rotating the vector (\bar{r}_{im2}) clockwise by the angle ($2\theta_{s4m}$).

Figure 12 shows how the new x-y components are determined for a vector which is originally oriented at an angle (ψ) and then rotated clockwise through an angle (δ). When computing (ψ), its quadrant must be taken into account.



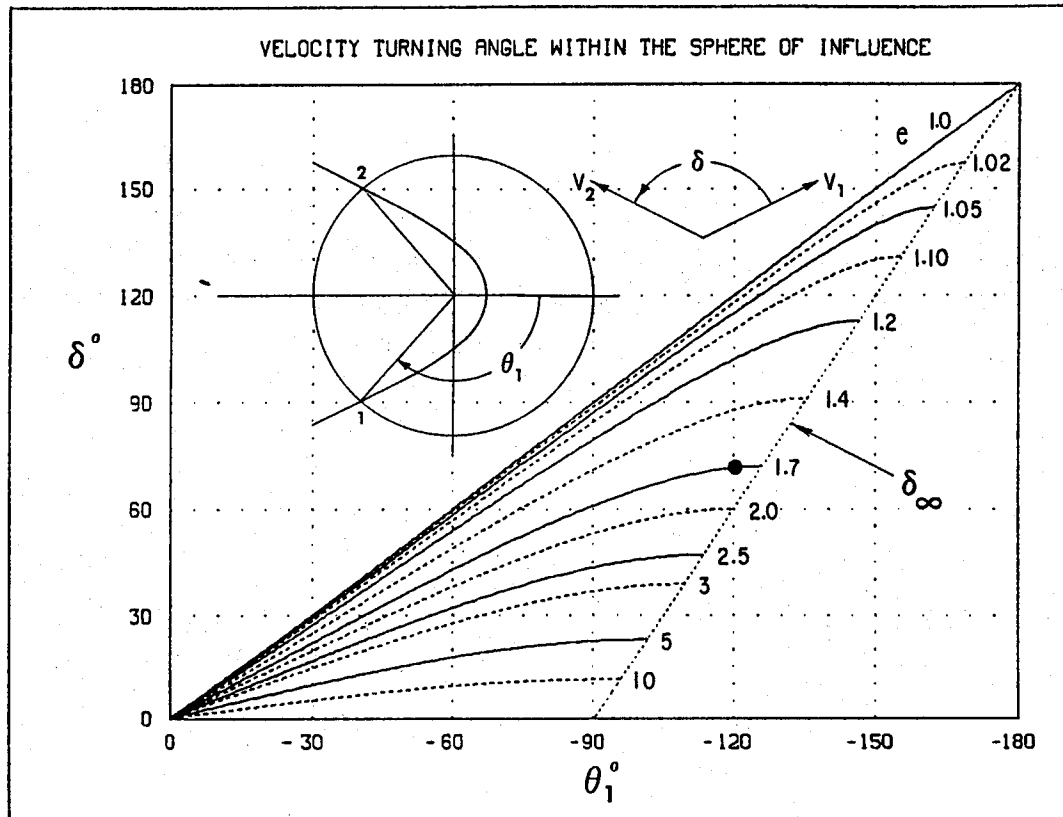
Also during hyperbolic passage, the relative velocity vector is rotated. Again provided the scalar angular momentum (h_{24}) was originally of negative sign, the rotation is clockwise. The relative velocity vector at approach (\bar{v}_{s2m}) is thus rotated clockwise to form the relative velocity vector at departure (\bar{v}_{s4m}) from the lunar influence sphere. If a spacecraft approaches a central body from a distance of infinity, its relative velocity vector is deflected by an angle

$$\delta_{\infty} = 2 \sin^{-1}(1/e)$$

In a patched-conic condition, however, the radius at approach is finite. Since the central body is "turned off" whenever the spacecraft is outside the influence sphere, the velocity turning angle will be somewhat smaller than (δ_{∞}). Figure 13 relates the turning angle (δ) to the eccentricity and initial true anomaly, where the turning is limited to that which occurs within the sphere of influence. In the case of the lunar free-return trajectory, the spacecraft enters the lunar influence sphere with ($\theta = -119.8^\circ$) and ($e = 1.687$) as indicated by the dot on the figure. The corresponding turning angle is 72.18° , counter-clockwise in Figure 13, but clockwise in Figure 11 due to the orientation of the hyperbola.

The moon translates during hyperbolic passage. However, the axis of the hyperbola remains fixed in orientation. The time

Figure 13



group from perilune at point (3) to point (4) can be doubled to obtain the total dimensionless time in the lunar influence sphere. Then the time is dimensionalized, allowing calculation of the change in the moon's position during hyperbolic passage. The hyperbolic anomaly (F_4) corresponds to the moon-relative true anomaly (θ_{s4m}) and eccentricity (e_{24}).

$$\cosh F_4 = (e_{24} + \cos \theta_{s4m}) / (1 + e \cos \theta_{s4m})$$

$$\sinh F_4 = \sqrt{\cosh^2 F_4 - 1}$$

$$F_4 = \ln(\cosh F_4 + \sinh F_4)$$

$$T_4 = (e_{24} \sinh F_4 - F_4) / [2\pi(e_{24}^2 - 1)^{3/2}]$$

$$t_{24} = (2T_4) 2\pi h_{24}^3 / \mu_m^2$$

$$\theta_{m4} = \theta_{m2} + t_{24} (d\theta/dt)_m$$

Given the moon's true anomaly (θ_{m4}) at the point where the spacecraft leaves the lunar influence sphere, the lunar velocity vector in x-y components can be determined and added to the spacecraft relative velocity vector (\bar{v}_{s4m}) to obtain the earth-relative spacecraft velocity vector:

$$\bar{v}_{s4} = \bar{v}_{s4m} + \bar{v}_{m4}$$

(14)

Then the earth-relative spacecraft radius (\bar{r}_{s4}) is obtained by adding the earth-moon radius vector (\bar{r}_{m4}) to the moon-spacecraft vector (\bar{r}_{im4}). Thus the earth-relative angular momentum for the return trajectory is determined by the vector cross product:

$$\bar{h}_4 = \bar{r}_{s4} \times \bar{v}_{s4}$$

The angular momentum is converted to scalar form (h_4) and the earth-relative velocity group, radius group, energy group, and eccentricity for the return trip are calculated:

$$V_{s4} = v_{s4} h_4 / \mu_\phi$$

$$R_{s4} = r_{s4} \mu_\phi / h_4^2$$

$$E_4 = \frac{1}{2}(V_{s4}^2) - (1/R_{s4})$$

$$e_4 = \sqrt{2E_4 + 1}$$

Finally, the moon's true anomaly at injection (θ_{m1}) is determined by calculating, and then dimensionalizing, the time group from point (1) to point (2). The resulting time (t_{12}) is added to the time (t_{23}) to determine the outbound time to perilune. At perilune, the altitude is obtained by dimensionalizing the moon-relative radius group:

$$R_{s3m} = 1/(1+e_{24}) \text{ at perilune}$$

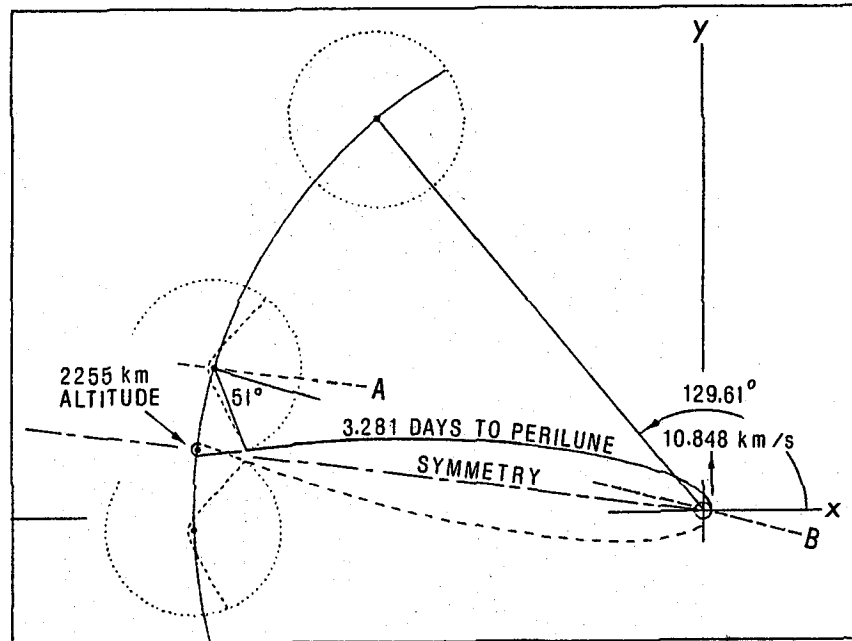
$$r_{s3m} = R_{s3m} h_{24}^2 / \mu_m$$

$$\text{Perilune altitude} = r_{s3m} - 1738 \text{ km}$$

Figure 14 presents the results of the analysis for the proper injection conditions ($v_{s1}=10.848$ km/s, $\theta_{m1}=129.61^\circ$). As might have been expected, the return trajectory is a mirror image of the outbound trajectory with respect to a line passing through the earth and the point of perilune. When the spacecraft is inside the lunar influence sphere, its earth-relative trajectory completes one end of a distorted "figure-8" shape. Since the axis (A) of the lunar passage hyperbola remains parallel to the line of symmetry, the axis passes through the earth at the point of perilune. Thus, the hyperbolic encounter with the moon does not change the energy of the spacecraft relative to the earth.

The major axis of the outbound elliptical transfer resides on the x-axis. That of the return ellipse (axis B) is inclined to the x-axis. Since the point of injection resides on the x-axis and that of return perigee resides on axis (B), the round trip falls just short of closing the "figure-8" shape.

Figure 14
Injection Conditions and Symmetry
of Lunar Free-Return Trajectory



CONCLUSIONS

1. The dimensionless orbital parameters (R,V,E, and T) offer compact mathematical and graphical presentation of Keplerian orbital characteristics, as well as efficient analysis of conic and patched-conic orbits.
2. Numerical solution of Kepler's problem confirms the accuracy of the flight time predicted by the auxiliary anomalies, even at near-parabolic eccentricities.
3. When iterative methods, including those using the auxiliary anomalies, are unable to converge on a solution to Kepler's problem, numerical integration offers a reliable, non-iterative solution.
4. Patched-conic orbits can be conveniently analyzed with the aid of Cartesian vector operations on the dimensional orbital parameters (r) and (v).

REFERENCES

1. Roger Bate, D.Mueller, and J.E.White, Fundamentals of Astrodynamics, Dover Publications, Inc., New York, 1971, pp. 16-29, 187-191.
2. Marshall H. Kaplan, Modern Spacecraft Dynamics and Control, John Wiley & Sons, New York, 1976, pp.91-96.

ACKNOWLEDGEMENT

The following individuals do not necessarily endorse the contents of this paper, but their assistance is greatly appreciated:

Dr. Vladimir Chobotov, of Aerospace Corporation, for a preliminary review and helpful suggestions

David Miller and Wayne Hurwitz, both of Northrop Corp., for development of the computer plotting system used for most of the figures.

APPENDIX 1
DERIVATION OF CONIC-SECTION DIMENSIONLESS PARAMETERS

Conic-Section Orbit Parameters

- μ Product of the central-body mass (M) and universal gravitational constant (G)
- r Radius from the mass center of the central body to that of the satellite
- θ True anomaly, or angle from closest passage (periapsis)
- v Magnitude of the velocity
- γ Direction (flight-path angle) of the velocity
- h Angular momentum (per unit satellite mass) about the central body
- t Time from periapsis to the true anomaly, θ
- ϵ Orbital energy per unit satellite mass

Conic-Section Orbital Equations (Ref. 1, p.16-29, p.187)

- 1) Radius $r = (h^2/\mu)/(1+e\cos\theta)$
- 2) Velocity $v = \sqrt{2(\epsilon + \mu/r)}$
- 3) Flight-path angle $\gamma = \cos^{-1} (h/rv)$
- 4) Angular momentum $h = rv \cos \gamma$
- 5) Energy $\epsilon = \mu^2(e^2-1)/2h^2 = v^2/2 - \mu/r$
- 6) Time from periapsis $t = (h^3/\mu^2) \int_0^\theta \frac{d\theta}{(1+e\cos\theta)^2}$

Appendix 1, continued
The Dimensionless Parameters

Equations (1-6) are now manipulated to yield the dimensionless quantities of equations (7-12), using upper-case symbols to designate non-dimensionality:

- 7) Dimensionless Radius, R $r\mu/h^2 = 1/(1+\text{ecos}\theta)$
- 8) Dimensionless Velocity, V using (1,2, and 5) $vh/\mu = \sqrt{1+e^2+2\text{ecos}\theta}$
- 9) Flight-Path Angle, $\cos \gamma = (h/rv) = 1/RV$
- 10) Dimensionless Angular Momentum, H $RV\cos \gamma = 1$
- 11) Dimensionless Energy, E using (5) or (7,8) $\epsilon h^2/\mu^2 = v^2/2 - 1/R = (e^2-1)/2$
- 12) Dimensionless Time, T from Periapsis $t\mu^2/2\pi h^3 = (1/2\pi) \int_0^\theta \frac{d\theta}{(1+\text{ecos}\theta)^2}$
- 13) Differentiate (12): $d\theta/dT = 2\pi(1+\text{ecos}\theta)^2$

Relate (T) to the auxiliary anomalies:

$$\begin{array}{l}
 14) \text{ For } e < 1, \quad T = \frac{\epsilon - e \sin \epsilon}{2\pi(1-e^2)^{3/2}} \quad \longrightarrow \quad \left\{ \begin{array}{l} \cos \epsilon = \frac{e + \cos \theta}{1 + \text{ecos}\theta} \\ \sin \epsilon = \frac{\sin \theta \sqrt{1-e^2}}{1 + \text{ecos}\theta} \end{array} \right. \\
 15) \text{ For } e = 1, \quad T = \frac{\tan(\theta/2)}{4\pi} + \frac{\tan^3(\theta/2)}{12\pi} \\
 16) \text{ For } e > 1, \quad T = \frac{e \sinh F - F}{2\pi(e^2-1)^{3/2}} \quad \longrightarrow \quad \left\{ \begin{array}{l} \cosh F = \cos \epsilon \\ \sinh F = \sqrt{\cosh^2 F - 1} \\ F = \ln(\cosh F + \sinh F) \end{array} \right.
 \end{array}$$

* For $\theta > \pi$, add to T the dimensionless period, $1/(1-e^2)^{3/2}$

** For $e=1$ or $e>1$, and θ negative, use positive θ and take the time as negative

APPENDIX 2

Application of the Dimensionless Groups Toward
The Iterative Solution of Kepler's Problem

Consider a satellite with velocity (v_0)=4 km/s at a flight-path angle (γ_0)=-60° and radius (r_0)=50,000 km from a central body with gravitational parameter (μ)=400,000 km³/s². Determine the position and velocity one hour later (subscript₁).

$$1) h = r_0 v_0 \cos \gamma_0 = 100,000 \text{ km}^2/\text{s}^2$$

$$2) V_0 = v_0 h / \mu = 1$$

$$3) R_0 = r_0 \mu / h^2 = 2$$

$$4) E = \frac{1}{2}(V_0^2) - (1/R_0) = 0$$

$$5) e = \sqrt{2E+1} = 1$$

$$6) \theta_0 = \cos^{-1}[(1/e)(1/R_0 - 1)] = -120^\circ \text{ (approaching periapsis)}$$

$$7) T_0 = -0.275665 \text{ from Appendix 1, Eq.(15)}$$

$$8) T_1 - T_0 = (t_1 - t_0) \mu^2 / 2\pi h^3 = 0.091674$$

9) To solve for the final true anomaly (θ_1) a first guess may be taken from Figure 10. The guess is designated θ_1'

$$\theta_1' = -110^\circ \text{ based on } T_1 = -0.275665 + 0.091674 = -0.183991$$

10) The corresponding time group, $T_1' = -0.190914$ from Eq.(15)

11) The desired value of T_1' is $T_1 = -0.183991$

Thus, the estimate θ_1' must be revised. The new guess is calculated from the local derivative ($d\theta/dT$) at θ_1' :

$$\theta_1'' = \theta_1' + (d\theta/dT)(T_1 - T_1')$$

$$\text{where } d\theta/dT = 2\pi(1 + e \cos \theta_1')^2 (360^\circ / 2\pi) = 155.857^\circ$$

$$\begin{aligned} \theta_1'' &= -110^\circ + 155.857^\circ [-0.183991 - (-0.190914)] \\ &= -108.921^\circ \end{aligned}$$

12) Repeat steps (10) and (11) for the following:

$$T_1' = -0.184173 \quad d\theta/dT = 164.383^\circ \quad \theta_1' = -108.891^\circ$$

$$T_1' = -0.183991 \quad \checkmark \quad \text{Thus, } \theta_1 = -108.891^\circ$$

13) Finally, $V_1 = \sqrt{1 + e^2 + 2e \cos \theta_1} = 1.16295 \quad v_1 = V_1 \mu / h = 4.6518 \text{ km/s}$

$$R_1 = 1 / (1 + e \cos \theta_1) = 1.47879 \quad r_1 = R_1 h^2 / \mu = 36970 \text{ km}$$

$$\gamma_1 = \cos^{-1}(1/R_1 V_1) = -54.445^\circ$$

(20)

APPENDIX 3
Application of Runge-Kutta
Numerical Integration to the
Solution of Kepler's Problem

Given the eccentricity (e), angular momentum (h), and initial true anomaly (θ_0) in a conic orbit, the change in orbital position during a time interval ($t_1 - t_0$) can be determined by numerical integration of the dimensionless derivative:

$$d\theta/dT = 2\pi(1+e\cos\theta)^2$$

Working with degrees, rather than radians, this becomes:

$$d\theta/dT = 2\pi(1+e\cos\theta)^2(360^\circ/2\pi) = 360^\circ(1+e\cos\theta)^2$$

The time interval is non-dimensionalized as follows:

$$T_1 - T_0 = (t_1 - t_0) \mu^2 / 2\pi h^3$$

Ordinarily, the time datum is zero at periapsis. However, the datum may arbitrarily be set to zero at the initial true anomaly. Then the numerical integration over (T) is terminated when (T) reaches ($T_1 - T_0$). The time group interval ($T_1 - T_0$) may be broken into constant or variable increments of (ΔT). For a given integration step, the gain ($\Delta\theta$) in true anomaly is calculated with the Runge-Kutta method as follows:

$$\Delta\theta_a^\circ = (d\theta/dT)_a^\circ \Delta T = 360^\circ(1+e\cos\theta_a)^2 \Delta T^*$$

$$\theta_b = \theta_a + \frac{1}{2}\Delta\theta_a$$

$$\Delta\theta_b = (d\theta/dT)_b \Delta T = 360^\circ(1+e\cos\theta_b)^2 \Delta T$$

$$\theta_c = \theta_a + \frac{1}{2}\Delta\theta_b$$

$$\Delta\theta_c = (d\theta/dT)_c \Delta T = 360^\circ(1+e\cos\theta_c)^2 \Delta T$$

$$\theta_d = \theta_a + \Delta\theta_c$$

$$\Delta\theta_d = (d\theta/dT)_d \Delta T = 360^\circ(1+e\cos\theta_d)^2 \Delta T$$

$$\text{Finally, } \Delta\theta = (1/6)(\Delta\theta_a + 2\Delta\theta_b + 2\Delta\theta_c + \Delta\theta_d)$$

At the very first step, $\theta_a = \theta_0$ and on the next step, $\theta_a = \theta_0 + \Delta\theta$. At the end of the very last step, $\theta_a + \Delta\theta = \theta_1$

* Computer evaluation of the cosine requires that (θ) be in radians.